The Korean Journal of Ceramics, 5[4] 357-362 (1999)

Characteristics of ZnO Varistors with Praseodymium Oxide

Sang Ki Lee, Sung Gurl Cho and Young Jae Shim*

Dept. of Electronic Materials Engr. and Advanced Materials Research Institute, Gyeongsang National University, Chinju, Gyeongnam 660-701, Korea
**Dept. of Inorganic Materials Engr. and Advanced Materials Research Institute, Gyeongsang National University, Chinju, Gyeongnam 660-701, Korea*
(Received September 23, 1998)

ZnO varistors containing cobalt, praseodymium and calcium oxides were prepared. The current-voltage characteristics and microstructures of the specimens were investigated with respect to calcium addition and sintering temperature. The potential barrier heights and the carrier densities were estimated from C-V relations. The compatibility of Ag-Pd as an internal electrode for multilayer chip varistor was also examined

Key words: Pr, ZnO, Ca, Varistor, Electrical properties, Microstructure

I. Introduction

ZnO varistors are polycrystalline ceramic devices composed of mainly ZnO, and varistor forming component such as bismuth oxide or praseodymium oxide, and various additive oxides. Highly nonlinear current-voltage characteristics of the ZnO varistors make them as important electric devices for protecting electric circuits.[1-5]

Most of commercial varistors contain bismuth oxide as a varistor forming component and show complicated microstructures. The drawbacks of bismuth oxide are its high volatility and reactivity with metal in liquid state. Especially the latter is a serious problem for producing multilayer type varistors using internal electrodes. The praseodymium oxide is an alternative replacing bismuth oxide as a varistor forming component.[6] However, ZnO-Pr_6O_{11} binary composition has a eutectic temperature near 1380°C which is much higher than melting temperature of bismuth oxide, 860°C, results in approximately 100°C higher sintering temperature of Pr-ZnO varistors than Bi-ZnO.[7]

In the present work the effect of calcium oxide on the microstructure and electrcial properties of ZnO-Pr_6O_{11}-Co_3O_4 basic composition was investigated with respect to sintering temperature and calcium oxide content.

II. Experimental Procedure

Conventional mixed oxide ceramic processing was used to prepare specimens. The chemical compositions of the specimens are 0.7 at% Pr_6O_{11}, 5.0 at% Co_3O_4, CaO (0, 0.2, 0.4, 0.6, 0.8 and 1.0 at%) and remaining ZnO. Reagent grade ZnO, Pr_6O_{11}, Co_3O_4 and $CrCO_3$ were mixed using a ball mill with methanol and zirconia balls. The powder was calcined at 1000°C for 2 hours and ball milled again. Next the powder was granulated by passing through a sieve after mixing with PVA solution using an alumina mortar and pestle. Disc shaped green compacts with diameter of 15 mm were uniaxially pressed and sintered at 1200, 1250 and 1300°C for one hour in an ambient atmosphere. The sintered specimens were cooled in the furnace which was shut off after completion of the soak time.

Apparent densities of all sintered specimens were measured to check the degree of densification. The fracture surfaces of the specimens were polished and thermally etched to observe the microstructure using an optical microscope (EPIPHOT-200, NIKON, Tokyo, Japan) and a scanning electron microscope (JSM-6400, JEOL, Tokyo, Japan). The surfaces of as fired specimens were also examined using the scanning electron microscope. Also the distribution of Ca was investigated using a field-emission type SEM (S-4200, Hitachi, Japan) equipped with EDS (Sigma MS2, Kevex, U.S.A). Average grain sizes of the specimens were obtained using the linear intercept method.

For electrical contact, both sides of the specimens were coated with In-Ga after polishing with SiC abrasive paper. Current-voltage characteristics were obtained using a I-V meter (Keitheley 237 High voltage source measure unit, Keithley Instruments, Cleveland, U.S.A) and nonlinear coefficients were determined from the slopes in the current density range of 1.0-10 mA/cm^2. The C-V analysis were conducted using a LF impedance analyzer (HP4192A, Hewlett Packard, Sandiego, U.S.A) at 10 kHz and 0-40 V internal bias. The carrier concentrations and the barrier heights of the specimens were calculated from the slopes of the C-V plots and the intercepts respectively using equations (1) and (2).[8]

$$\left(\frac{1}{C}-\frac{1}{2C_o}\right)^2 = \frac{2}{q\varepsilon N_d}(\Phi_b + V) \quad (1)$$

$$\frac{1}{C_o} = 2\left(\frac{2\Phi_b}{q\varepsilon N_d}\right)^{1/2} \quad (2)$$

where C is the capacitance per unit grain boundary area, C_o is the capacitance at V=0, q is the electron charge, ε is the permittivity of ZnO ($8.5\varepsilon_o$), N_d is the donor density of ZnO grain, Φ_b is the built-in potential, and V is the applied voltage.

The multilayer chip varistors with 0.6 at% Ca were fabricated using the tape casting process. The Pd-Ag internal electrodes were screen printed on the ceramic tapes and laminated prior to firing at 1200°C for 1 hour. The microstructure of the cross-section and I-V characteristic were investigated using the scanning electron microscope and the I-V meter, respectively.

III. Results and Discussion

The apparent densities of the sintered specimens were in the range of 5.2-5.5 g/cm^3. Comparing with the theoretical density of ZnO, 5.6 g/cm^3, these are 93-98% relative densities. The density increased with the sintering temperature, but its dependence on the Ca content is complicated as shown in Fig. 1. The highest densities were obtained for the specimens containing 0.6% Ca, and further increase of Ca content lowered the density. Since Ca is lighter than Zn, simple replacement of Zn with Ca will lower the density. It is presumed that the addition of appropriate amount of Ca promotes densification of the samples. The adverse effect of high Ca addition was also observed in the electrical properties of the specimens, which will be discussed later.

The optical micrographs of the specimens containing 0.4% Ca given in Fig. 2 shows clearly the increase of grain size with the sintering temperature. The same trend was observed for the specimens with different amount of Ca. The average grain sizes of the specimens sintered at 1200°C were in the range of 3.5-4.6 μm depending upon the Ca content, while those sintered at 1250°C and 1300°C were 7.6-17.0 μm and 20.5-31.3 μm, respectively.

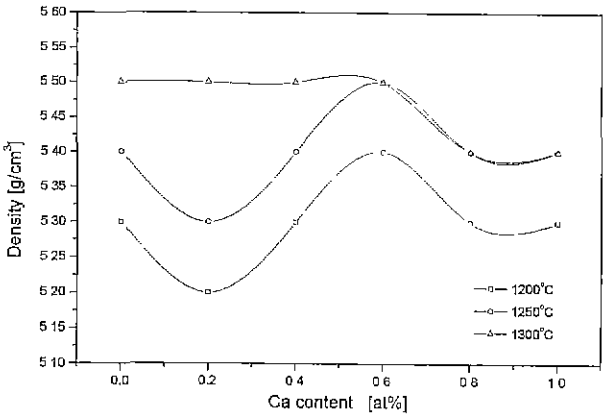

Fig. 1. Densities of the specimens sintered at 1200, 1250 and 1300°C for 1 h as a function of Ca content

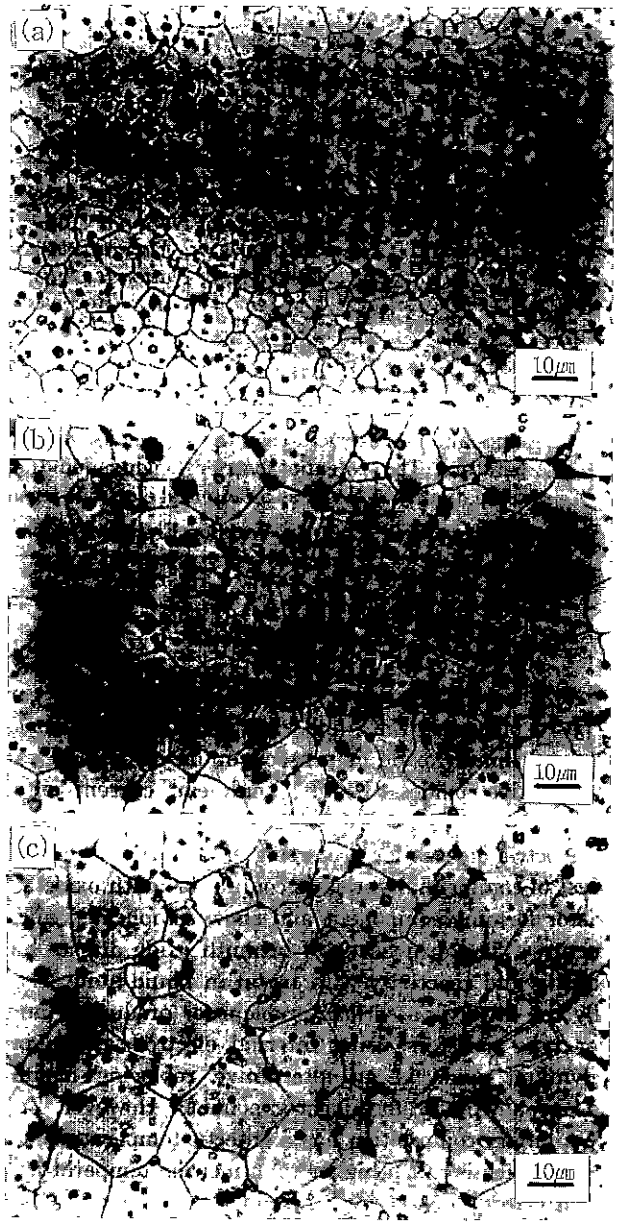

Fig. 2. Optical micrographs of the specimens containing 0.4% Ca and sintered at; (a) 1200°C, (b) 1250°C and (c) 1300°C for 1 h.

The average grain size increased with Ca content as shown in Fig. 3 for the specimens sintered at 1250°C for 1 h. In Fig. 4 the average grain sizes of the specimens sintered at different temperatures were plotted as a function of Ca content. On the contrary to the slight increase of the grain size with Ca content for the specimens sintered at 1200°C, a significant increase is observed for those sintered at 1250 and 1300°C. The reason for this difference can be understood from the SEM micrographs of the as fired surface of the specimens containing 0.6% Ca shown in Fig. 5. The liquid phase mainly consisting of praseodymium oxide was observed from the SEM image along the grain boundaries for the specimens sintered at 1250 and

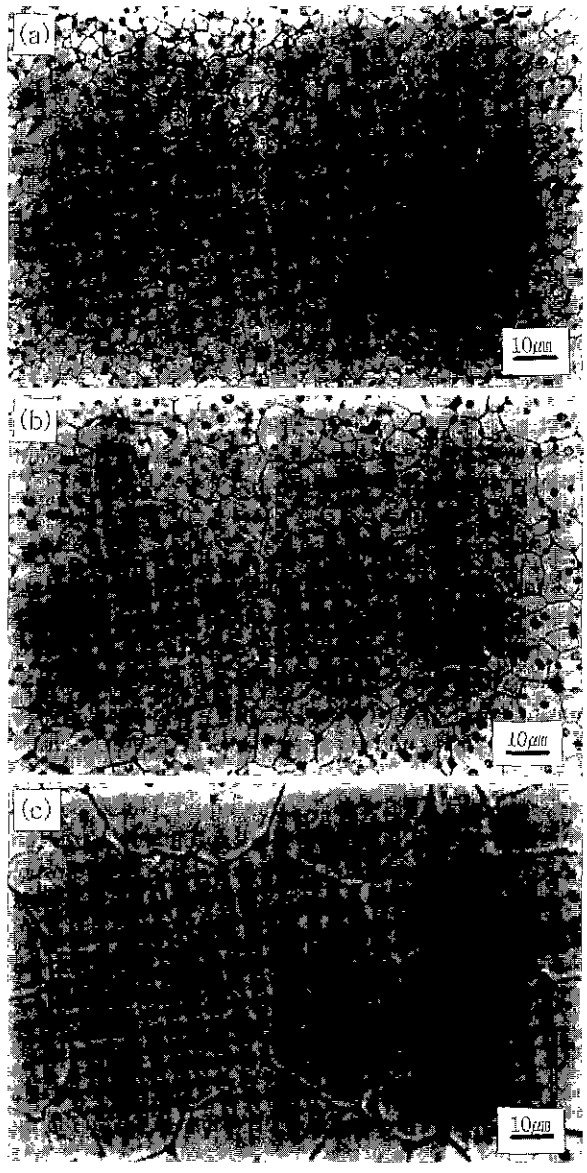

Fig. 3. Optical micrographs of the specimens sintered at 1250°C for 1 h which contain; (a) 0.2% Ca, (b) 0.6% Ca and (c) 1.0% Ca.

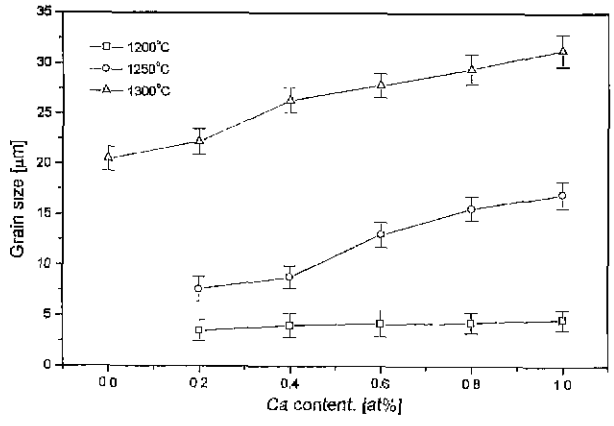

Fig. 4. Average grain sizes of the specimens sintered at 1200, 1250 and 1300°C as a function of Ca content.

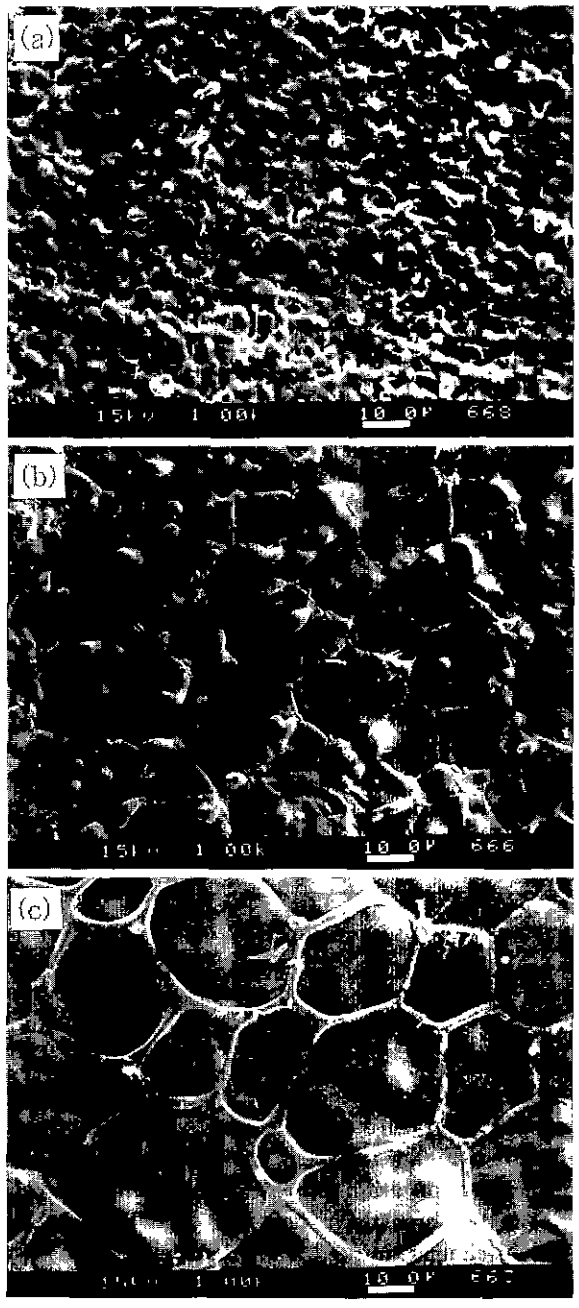

Fig. 5. SEM micrographs of as-fired surface of the specimens containing 0.6% Ca and sintered at; (a) 1200°C, (b) 1250°C and (c) 1300°C for 1 h.

1300°C, while discrete second phase is found at the grain boundaries for those sintered at 1200°C. The reported data for the liquid phase formation temperature of ZnO-Pr_6O_{11}-Co_3O_4 ternary composition is higher than 1280°C.[9] Therefore it is concluded that the addition of Ca decreases the liquid phase formation temperature and pronounced increase of grain size for the specimens sintered at 1250 and 1300°C is resulted from liquid phase sintering.

The current-voltage curves of the specimens did not show a specific trend with respect to Ca content, but a poor result was obtained for the sample with 1.0% Ca as

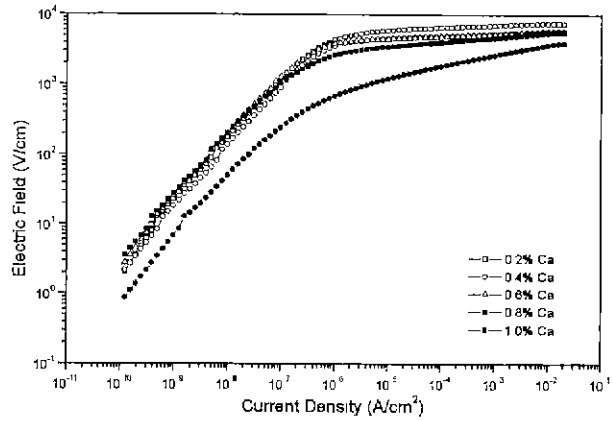

Fig. 6. I-V curves of the specimens with various Ca content and sintered at 1200°C for 1 h.

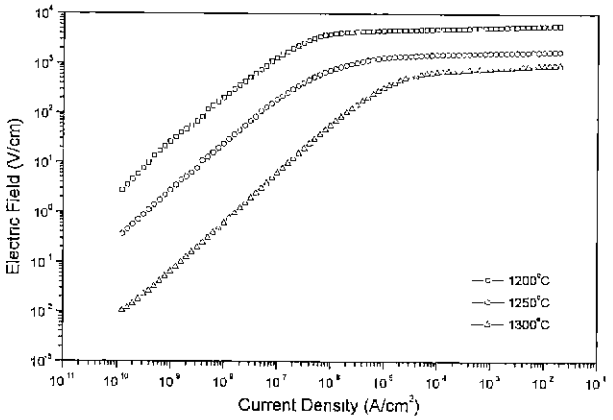

Fig. 7. I-V curves of the specimens containing 0.6% Ca and sintered at 1200, 1250 and 1300°C for 1 h.

shown in Fig. 6 for those sintered at 1200°C. The effect of sintering temperature on the current-voltage curve is well exhibited in Fig. 7 for the samples containing 0.6% Ca. The increase of grain size with sintering temperatue results in low breakdown field and high leakage current for the specimens sintered at higher temperature.

The nonlinear coefficients, breakdown voltage per grain boundary and leakage current measured for the specimens are summarized in Table 1. For the samples sintered at 1200 and 1250°C the nonlinear coefficient, the

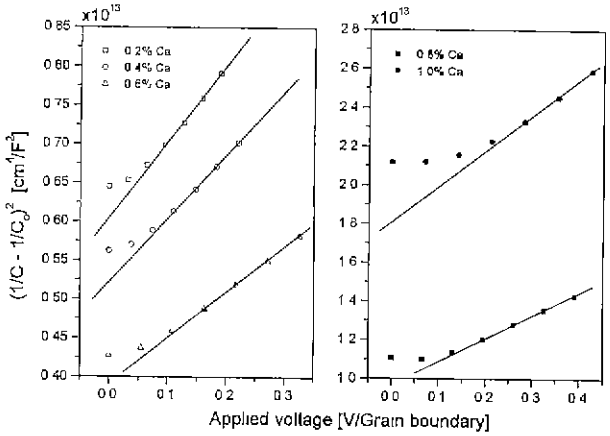

Fig. 8. $(1/C-1/2C_0)^2$ vs applied voltage per grain boundary curves for the specimens sintered at 1250°C for 1 h.

breakdown voltage per grain boundary and the leakage current changed significantly above 0.8% Ca. However, those measured for the specimens sintered at 1300°C did not show the same trend except the leakage current. The different effect of Ca content for the specimens sintered at 1200 and 1250°C and for those fired at 1300°C is attributable to the liquid phase formed along the grain boundaries. As shown in Fig. 5, the liquid phase completely surrounds the grains for the specimens sintered at 1300°C, which possibly makes any change in grain boundary property due to excess amount of Ca insignificant. The abrupt change observed for the specimens with Ca content higher than 0.8% was presumed to be due to the solubility limit of Ca. Therefore EDS associated with field-emission SEM was applied to investigate Ca segregation at the grain boundaries, but no specific signal from the grain boundary region was detected. The authors planned to use TEM for further investigation of grain boundary segregation.

The charge carrier density and the potential barrier heights were estimated from the plots of $(1/C-1/C_0)^2$ versus applied voltage per grain boundary as shown in Fig. 8 for the specimens sintered at 1250°C. The deviation of points from the linearity is observed in the low voltage range. The carrier density and the barrier heights obtained using C-V plot and equations (1) and (2) were

Table 1. Nonlinear Coefficients and Breakdown Voltage per Grain Boundary for ZnO Varistors

samples	1200°C			1250°C			1300°C		
	α	E_b[†](V)	L_c[‡](μA)	α*	E_b[†](V)	L_c[‡](μA)	α*	E_b[†](V)	L_c[‡](μA)
0% Ca	-	-	-	-	-	-	16	2.3	50.0
0.2% Ca	28	2.4	6.0	22	2.1	16.0	20	2.5	48.0
0.4% Ca	28	2.2	4.0	26	2.2	4.9	19	2.4	71.0
0.6% Ca	30	2.2	2.0	34	2.0	8.0	18	2.3	67.0
0.8% Ca	15	2.0	29.0	12	1.7	74.0	11	2.0	156.0
1.0% Ca	7	1.3	250.0	7	1.3	230.0	18	2.3	88.0

*Nonlinear coefficient (α): Measured at 10^{-3}~10^{-2}A/cm². †Breakdown voltage per grain boundary (E_b). Measured at 10^{-3}A/cm².
‡Leakage current (L_c). Measured at 80% voltage of 10^{-3}A/cm².

Table 2. Carrier Densities and Barrier Heights of ZnO Varistors Estimated from C-V Plots

samples	1200°C		1250°C		1300°C	
	Carrier density (cm^{-3})	Barrier height (eV)	Carrier density (cm^{-3})	Barrier height (eV)	Carrier density (cm^{-3})	Barrier height (eV)
0% Ca	-	-	-	-	1.8×10^{18}	1.3
0.2% Ca	1.2×10^{18}	1.6	1.9×10^{18}	0.8	2.1×10^{18}	1.3
0.4% Ca	1.4×10^{18}	1.6	2.0×10^{18}	1.0	1.4×10^{18}	1.4
0.6% Ca	1.6×10^{18}	1.6	2.7×10^{18}	1.0	1.4×10^{18}	1.4
0.8% Ca	1.4×10^{18}	2.6	1.7×10^{18}	1.3	9.7×10^{17}	1.5
1.0% Ca	5.0×10^{17}	1.3	1.3×10^{18}	1.8	8.1×10^{17}	2.0

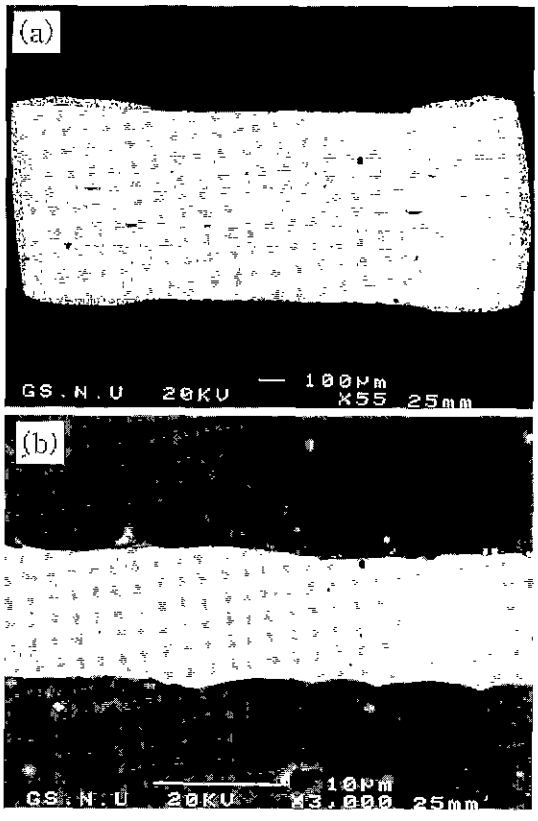

Fig. 9. Back-scattered mode SEM micrographs for the multilyer chip varistor containing 0.6% Ca and sintered at 1200°C.

summarized in Table 2. For the specimens sintered at 1200 and 1250°C the carrier density increased with Ca content up to 0.6%, implying the substitution of Zn^{2+} (0.74) with Ca^{2+} (0.99) enhancing the donor defects. Again the decrease of the carrier density for the samples with excessive Ca content, 0.8% and 1.0%, was observed. The barrier heights estimated for the specimens did not show specific relation with Ca content nor the sintering temperature.

The multilayer chip varistor containing 0.6% Ca were prepared using the tape casting process and Pd-Ag internal electrode. The cross-section and the current-voltage curve of the multilayer varistor sintered at 1200°C are shown in Fig. 9 and 10, respectively. Good adhesion and no reaction between the ceramic tape and the electrode were achieved.

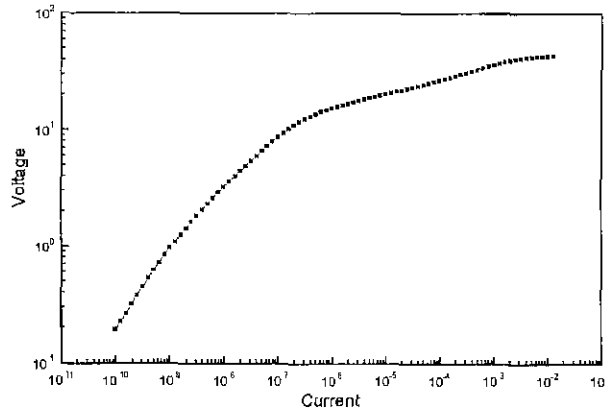

Fig. 10. I-V curve for the multilyer chip varistor containing 0.6% Ca and sintered at 1200°C.

IV. Conclusions

The microstructure and electrical properties of ZnO varistors containing Pr_6O_{11}, Co_3O_4 and CaO were investigated with respect to Ca content and the sintering temperature. The average grain size increased with Ca content, while the maximum density was obtained when 0.6% Ca was added. The addition of Ca also lowered the liquid phase formation temperature of ZnO-Pr_6O_{11}-Co_3O_4 ternary composition. The electrical properties including nonlinear coefficient, leakage current and carrier density were improved by the addition of Ca up to 0.6%. However, when the Ca content exceeded 0.8%, those properties became poor.

Acknowledgment

Present work is supported by the academic research of Ministry of Education, Republic of Korea. The authors would like to thank Mr. Kyoung-Taik Park of Amotron Co., Kimpo, Korea for fabricating the multilayer chip varistor.

References

1. K. Eda, "Zinc Oxide Varistors," *IEEE Electrical Insulation Magazine*, **5**(6), 28-41 (1989).
2. T. K. Gupta, "Application of Zinc Oxide Varistors," *J. Am.*

Ceram. Soc., **73**(7). 1817-40 (1990).
3. M. Matsuoka, "Nonohmic Properties of Zinc Oxide Ceramics," *Jpn J. Appl. Phys.* **10**, 736-746 (1970).
4. Y.-S. Lee. K.-S. Liao and T.-Y. Tseng, "Microstructure and Crystal Phases of Praseodymium Oxides in Zinc Oxide Varistor Ceramics," *J. Am Ceram. Soc.*, **79**(9), 2379-84 (1996).
5. L. M. Levinson and H. R. Philipp, "Zinc Oxide Varistors-A Review," *Am. Ceram. Soc. Bull.*, **65**(4), 639-646 (1986).
6. K. Mukae. "Zinc Oxide Varistors with Praseodymium Oxide" *Am. Ceram. Soc. Bull.*, **66**(9), 1329-1331 (1987).
7. S.-Y. Chun, N. Wakiya, H. Funakubo, K. Shinozaki and N. Mizutani, "Phase Diagram and Microstructure in the ZnO-Pr_2O_3 System," *J Am. Ceram Soc.*, **80**(4) 995-98 (1997).
8. K. Mukae, K. Tsuda, and I. Nagasawa, "Capacitance-vs-Voltage Characteristics of ZnO Varistors," *J. Appl. Phys.*, **50**(6). 4475-76 (1979).
9. A. B. Alles and V. L. Burdick. "Compositional Effects on the Liquid-Phase Sintering of Praseodymium Oxide-Based Zinc Oxide Varistors," *J Am. Ceram. Soc.*, **76**(8), 2098-102 (1993).